Geophysical Research Letters

RESEARCH LETTER
10.1029/2019GL085679

Key Points:
- Atmospheric model experiments aid causal interpretation of links between Arctic sea ice and midlatitude winter atmospheric circulation
- Observed links between autumn Barents-Kara sea ice and the winter North Atlantic Oscillation is largely explained by internal variability
- Observed links between autumn Barents-Kara sea ice and the winter Aleutian Low appears to originate from tropical SST and rainfall changes

Supporting Information:
- Supporting Information S1

Correspondence to:
J. L. Warner,
Jw773@exeter.ac.uk

Citation:
Warner, J. L., Screen, J. A., & Scaife, A. A. (2020). Links between Barents-Kara sea ice and the extratropical atmospheric circulation explained by internal variability and tropical forcing. *Geophysical Research Letters*, *47*, e2019GL085679. https://doi.org/10.1029/2019GL085679

Received 4 OCT 2019
Accepted 18 DEC 2019
Accepted article online 19 DEC 2019

©2019. American Geophysical Union. All Rights Reserved.

Links Between Barents-Kara Sea Ice and the Extratropical Atmospheric Circulation Explained by Internal Variability and Tropical Forcing

J. L. Warner[1], J. A. Screen[1], and A. A. Scaife[1,2]

[1]College of Engineering, Mathematics and Physical Sciences, University of Exeter, Exeter, UK, [2]Met Office Hadley Centre, Exeter, UK

Abstract Changes in Arctic sea ice have been proposed to affect midlatitude winter atmospheric circulation, often based on observed coincident variability. However, causality of this covariability remains unclear. Here, we address this issue using atmospheric model experiments prescribed with observed sea surface temperature variations and either constant or time-varying sea ice variability. We show that the observed relationship between late-autumn Barents-Kara sea ice and the winter North Atlantic Oscillation can be reproduced by simulated atmospheric internal variability but is not simulated as a forced response to sea ice. Observations and models suggest reduced sea ice is linked to a weaker Aleutian Low. We show that simulated Aleutian Low variability is correlated with observed sea ice variability even in simulations with fixed sea ice, implying that this relationship is not incidental. Instead, we suggest that covariability between sea ice and the Aleutian Low originates from tropical sea surface temperature and rainfall variations and their teleconnections to the extratropics.

Plain Language Summary Recent dramatic changes in Arctic sea ice due to climate change have been linked to changes in weather patterns across the Northern Hemisphere. Many studies have proposed such links, but correlation does not necessarily imply causality. Here, we explore the causality of this link using atmospheric models run with observed sea surface temperature variations and either constant or time-varying sea ice. We find that changes in weather patterns over the Atlantic that are correlated with sea ice variations are not caused by changes in sea ice. Instead, the correlation appears to be an incidental occurrence due to internal atmospheric variability. Additionally, we find that changes in weather patterns over the North Pacific, which are also correlated with sea ice variations, are reproduced in model experiments with no knowledge of these sea ice variations. In this case, the correlation appears to arise due to a third factor: rainfall variations over the tropical Pacific Ocean, which can affect midlatitude weather irrespective of sea ice changes.

1. Introduction

The loss of Arctic sea ice in recent decades has been widely linked to variability in midlatitude weather, including aspects such as the jet stream (Francis & Vavrus, 2015), cold air outbreaks (Collow et al., 2019; Liu et al., 2012), sudden stratospheric warmings (Kim et al., 2014), and the North Atlantic Oscillation (NAO) (Petoukhov & Semenov, 2009). There is, however, little consensus on how interannual variability and trends in Arctic sea ice affect midlatitude weather variability. For example, modeling studies produce a spectrum of responses in the NAO due to Arctic sea ice loss, with no consensus even on the sign of the response (Smith et al., 2017). Reasons for these discrepancies may include a large component of internal variability masking forced signals (Screen, 2017), differing background states of the climate models (Smith et al., 2017), or varying representations of stratosphere-troposphere coupling (De & Wu, 2019). Given the rapid decline in Arctic sea ice, furthering our understanding of the relationship between Arctic sea ice and the midlatitude circulation is imperative for societal adaptation to climate variability and change.

Interannual sea ice variability is nonuniform across the Arctic and the locations of greatest variability are dependent on season. In late autumn/winter, variability is particularly pronounced in the Barents and Kara (BK) Seas (Onarheim et al., 2018). Many studies have related autumn variability and loss of BK sea ice to winter midlatitude circulation patterns (e.g., Vihma, 2014; Sun et al., 2015; Zhang et al., 2018; Liptak & Strong, 2014), either via a stratospheric pathway (Kelleher & Screen, 2018; McKenna et al.,

2018) through modulation of upward planetary wave propagation into the stratosphere (Kim et al., 2014). This can weaken the polar vortex, exerting a lagged tropospheric influence later in winter (Kidston et al., 2015); or via a tropospheric route through deepening the Icelandic node of the NAO regionally due to surface heating anomalies related to sea ice loss (Orsolini et al., 2012; Cassano et al., 2014).

Some studies have sought to exploit connections between interannual sea ice variability and the extratropical atmospheric circulation for seasonal predictions of the winter NAO. Both Hall et al. (2017) and Wang et al. (2017) used autumn BK sea ice to construct empirical predictions of the winter NAO, and Scaife et al. (2014) identified an apparent dependence of dynamical winter NAO forecasts to the sea ice conditions in the Kara Sea during November. However, while Arctic sea ice may serve as a good statistical predictor of the winter NAO, or of the spread in dynamical forecasts, this does not necessarily imply the relationship is causal. While advanced statistical tools have been developed, such as causal network analysis (Runge et al., 2015), which indicate a causal link between BK sea ice and the Arctic Oscillation (Kretschmer et al., 2016), they are susceptible to limitations such as the subjective inclusion (or not) of all important mediating processes and assumptions of stationarity (Runge et al., 2015). The latter may be especially problematic for the relationship between autumn BK sea ice and the winter NAO (Kolstad & Screen, 2019).

Separately, variability in the tropics has also been linked to Arctic sea ice variability through poleward heat fluxes and changes in the radiation budget (Baxter et al., 2019; Lee, 2012; Lee et al., 2011). Such teleconnection is mooted to be triggered by the El Niño–Southern Oscillation (ENSO) or the Madden-Julian Oscillation (Henderson et al., 2014), through changes in tropical convection and upper-level divergence that can generate poleward propagating Rossby waves (Sardeshmukh & Hoskins, 1988; Scaife et al., 2017; Trenberth et al., 1998). Rossby wave dynamics connecting tropical rainfall variability and the winter midlatitude circulation are well established (e.g., Cassou, 2008; Knight et al., 2017; Toniazzo & Scaife, 2006).

Given that tropical variability is known to influence the extratropical circulation, and potentially sea ice variability (e.g., Gong et al., 2017; Park et al., 2015; Woods et al., 2013; Woods & Caballero, 2016), we hypothesize that observed relationships between Arctic BK sea ice and the midlatitude winter circulation could be partially explained by a common driver: tropical variability. In this paper, we explore this hypothesis using both reanalysis and parallel multimodel atmospheric model experiments with and without sea ice variability.

2. Data and Methods

We use ERA-Interim (ERA-I) (Dee et al., 2011) monthly-mean mean sea level pressure (MSLP) fields spanning the period 1980–2015. We focus on atmospheric conditions in winter defined here as December to February average. We define the NAO index by subtracting the winter MSLP over Iceland (16–25°W, 63–70°N) from that over the Azores (20–28°W, 36–40°N), following Dunstone et al. (2016). To generate our BK sea ice time series, we use the Hadley Centre Sea Ice and Sea Surface Temperature data set Version 2 (Titchner & Rayner, 2014) monthly-mean sea ice concentration in November for the period 1980–2015 and calculate the total ice-covered area where sea ice concentration is greater than 15% in the domain 10–100°E, 65–85°N. As a proxy for tropical atmospheric convection, we use precipitation fields from the Global Precipitation Climatology Project (Adler et al., 2003) over the period 1980–2015 and derive an index of September–October mean precipitation over the western tropical Pacific (110–140°E, 5°S to 25°N), following Scaife et al. (2017). Our motivation for using this region stems from work suggesting Madden-Julian Oscillation Phase 5–7 is particularly effective at stimulating planetary waves which can affect sea ice variability, both in summer and winter (Henderson et al., 2014), and is strongly linked to ENSO variability (Lee, 2012; Moon et al., 2011). The choice of September/October tropical rainfall, November BK sea ice, and December–February winter MSLP allows a lagged linear regression to be constructed.

For the model intercomparison, we use atmospheric model simulations from the Facility of Climate Assessments repository. This contains four models: GFSv2 (Saha et al., 2014), ECHAM5 (Roeckner et al., 2003), CAM4 (Neale et al., 2010), and CAM5.1 (Neale et al., 2010). For each model, 20 ensemble members are used, producing a multimodel ensemble of 80 members. We used the period 1980–2015 in line with the reanalysis. Two experiments were performed: one containing observed sea surface temperature (SST) variability and observed sea ice variability (hereafter $\mathrm{AMIP_{OBS}}$) and the other with observed nonpolar (SST) variability but climatological sea ice and polar SSTs (hereafter $\mathrm{AMIP_{CLIM}}$). Note that the

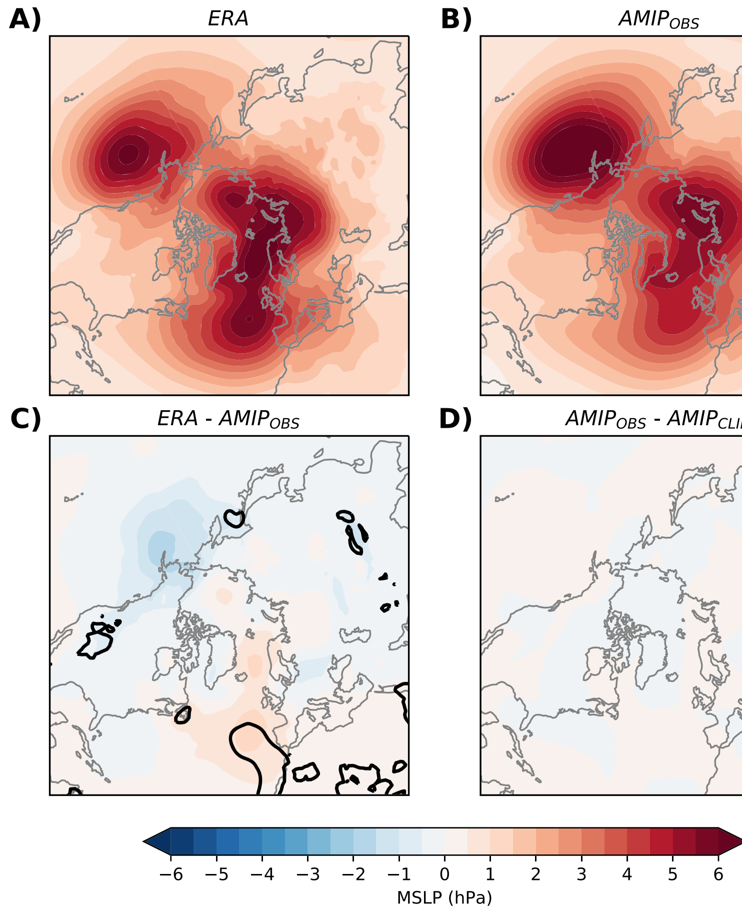

Figure 1. a) Standard deviation of interannual winter mean sea level pressure (MSLP) in ERA Interim. (b) Same as in (a), except for $AMIP_{OBS}$. Here the standard deviation is first calculated for each ensemble member individually and then averaged. (c) Difference between the standard deviation of winter MSLP in ERA Interim and $AMIP_{OBS}$. At each grid point, the standard deviation of MSLP is calculated for each member. Regions where reanalysis fall outside 5–95% range of the ensemble PDF are contoured. (d) Difference between the standard deviation of winter MSLP in $AMIP_{OBS}$ and $AMIP_{CLIM}$.

experiments differ only in their representation of polar sea ice and SSTs; both include the same extratropical and tropical SST variability. Sun et al. (2016) and Mori et al. (2019) used the same simulations to investigate the recent Eurasian cooling trend and its potential relationship to sea ice loss.

An additional experiment was performed to isolate the influence of ENSO (hereafter $AMIP_{ENSO}$). This comprises ECHAM5, CAM4, and GFSv2, with each model containing 20 ensemble members (total 60 members). This experiment was constructed through adding the global detrended leading empirical orthogonal function of SST anomalies onto the monthly varying climatological SSTs. The leading mode of variability is the ENSO pattern in the Pacific Ocean. More details, along with the loading pattern can be found in NOAA ERSL (2019). We note that while this experiment excludes observed interannual SST variability unrelated to ENSO, it contains observed sea ice variability.

3. Variability in Winter MSLP

Our first analysis verifies that the simulations capture interannual winter variability in MSLP similarly to reanalysis. The regions of maximum interannual variability (Figure 1a) are located in the Atlantic and Pacific storm tracks, and over the Arctic. Interannual variability across all members in $AMIP_{OBS}$ (Figure 1b) shows a similar spatial pattern and magnitude to that in ERA-I (Figure 1a), and the differences are small compared to the magnitude of MSLP variability itself (Figure 1c). The model therefore well simulates internal variability, but to further assess the importance of these small differences, we identified regions where the MSLP variance in reanalysis lied outside the 5–95% range of standard deviation values obtained from the individual ensemble members. Small regions over the Azores were identified where the magnitude of variability in the reanalysis were outside this 5–95% range (Figure 1a). However, similar-sized regions also occurred when we compared a single model realization to the distribution obtained from all members, and therefore, we cannot rule out that such differences are just a chance occurrence rather than indicative of model error.

We next compare the standard deviation of MSLP in $AMIP_{OBS}$ and $AMIP_{CLIM}$ to examine whether it is necessary to prescribe sea ice in order to simulate realistic MSLP variability. The differences in MSLP variance between simulations with observed time-varying and fixed climatological sea ice are minimal (Figure 1d), suggesting that sea ice (and polar SST) variability has little effect on interannual variability of winter MSLP, even in the Arctic. We next consider how well the simulations capture the observed interannual variability of the winter NAO. Here we use the multimodel ensemble-mean to extract the forced component of NAO variability. We perform a linear Pearson correlation on the two multimodel ensemble means, with the observed NAO index derived from ERA-Interim MSLP data. The multimodel ensemble-mean winter NAO index for $AMIP_{OBS}$ is weakly, but significantly, correlated with the ERA-I NAO index ($r = 0.33$, $p = 0.05$). We note that the differences between the models in this regard are small, with correlations of 0.2–0.3 for model-specific ensemble means. The multimodel ensemble-mean winter NAO index for $AMIP_{CLIM}$ is also weakly correlated with the observed NAO index ($r = 0.29$, $p = 0.09$). Although the latter correlation is weaker, it is not statistically different from the former correlation. This suggests that the modest model "skill" in reproducing the observed NAO originates from sources other than Arctic sea ice variability, such as nonpolar SST variability. The lack of any significant increase in skill in $AMIP_{OBS}$ compared to $AMIP_{CLIM}$ suggests the inclusion of variability in sea ice and polar SST's does not drive NAO variability, at least in these models. The limited NAO skill in the AMIP simulations is likely due to a lack of stratospheric initial conditions, which have been shown to be important in more sophisticated forecast systems (Nie et al., 2019).

4. November BK Sea Ice and the Subsequent Winter Circulation

We now turn to the relationship between autumn BK sea ice variability and the subsequent winter circulation, both in AMIP multimodel experiments and in reanalysis. By regressing observed November BK ice onto observed DJF sea level pressure at each grid point, we reveal a pattern that projects strongly onto the negative phase of the NAO. Additionally, increased MSLP across the Arctic and North Pacific in relation to low sea ice is found (Figure 2a). This observed relationship between low autumn sea ice and the negative NAO relationship has been well documented (Kim et al., 2014; Petoukhov & Semenov, 2009; Yang & Christensen, 2012), along with increased blocking over the BK seas and Eurasia in relation to low sea ice (Gastineau et al., 2017; Mori et al., 2014). We note that despite this strong projection onto the NAO, there is a large standard error about the regression coefficient in reanalysis, due to large variability and limited sample length (as discussed in Screen et al. (2017)).

Each member in the model ensemble contains internal variability as well as any forced response. Given a sufficiently large ensemble, the ensemble mean only retains the forced response as internal variability cancels out through averaging the ensemble members. To determine whether members can reproduce the NAO pattern and magnitude via internal variability, we repeat the regression of November BK sea ice onto the *individual* ensemble members and select the member with the strongest link to the NAO (see methods for the box used) (Figure 2b). This ensemble member well reproduces the negative NAO associated with reduced BK sea ice, consistent with the idea that the link could be apparent and due to internal variability. Nevertheless, the magnitude of this pattern is weaker to that found in reanalysis (Figure 2a), and there are regions where the observed regression coefficient lie outside the 5–95% confidence interval of regression coefficients calculated from each member separately (Figure 2a). As before, repeating this comparison but replacing observations with individual ensemble members generates apparent discrepancies of similar spatial extent in approximately 10% of cases (not shown). We therefore cannot reject the null hypothesis that apparent differences between the observed and simulated regression patterns are due to sampling uncertainty. That said, we are mindful of the caveat that the models may respond too weakly to surface forcing, for example, sea ice variability, even though they capture fairly well the observed MSLP variability, the so-called signal-to-noise paradox (e.g., Scaife & Smith, 2018).

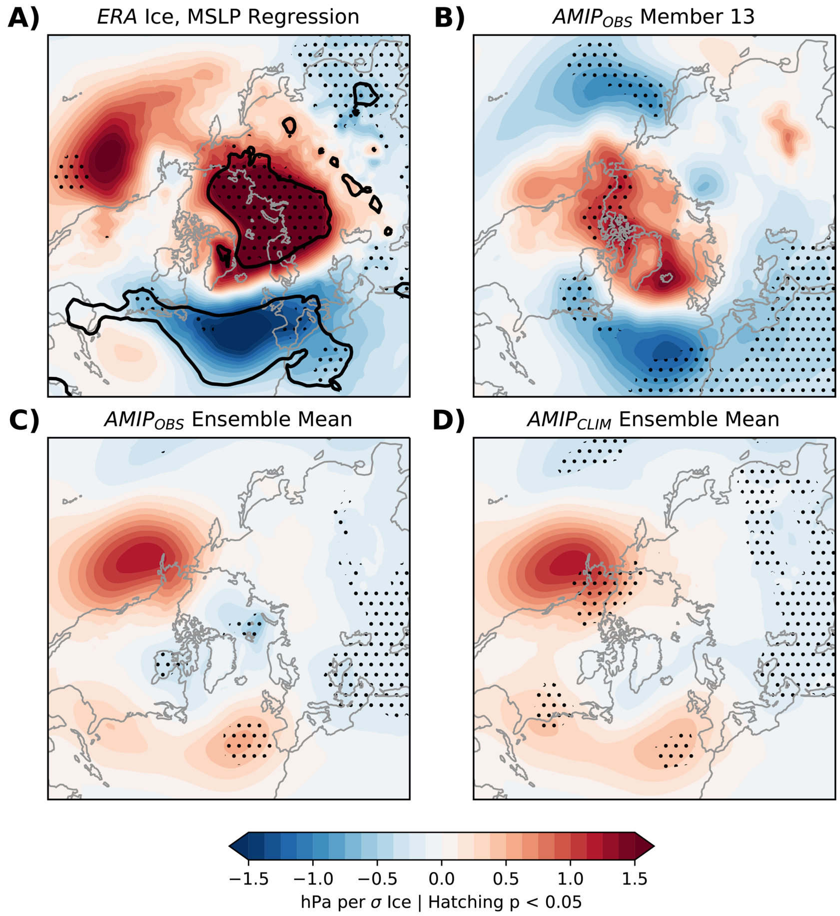

Figure 2. (a) Linear regression of standardized November Barents-Kara sea ice onto winter mean sea level pressure (MSLP) in ERA-Interim. Stippling is shown where the regression coefficient is statistically different from zero at the 95% confidence level. All regression coefficients have been multiplied by −1 to infer the relationship with low sea ice. Regions where the reanalysis regression coefficient falls outside the 5–95% confidence range of ensemble member regression coefficients is contained by a thick black line. (b) Same as the regression in (a), except for AMIP$_{\mathrm{OBS}}$ Member 13, selected because it was the realization with a regression pattern that projected mostly strongly onto the negative phase of the North Atlantic Oscillation. (c) Same as in (b), except for AMIP$_{\mathrm{OBS}}$ ensemble mean. (d) Same as in (b), except for the AMIP$_{\mathrm{CLIM}}$ ensemble mean.

Next we explore the relationship between observed November BK ice and the multimodel ensemble mean in both AMIP experiments to identify forced relationships. The regression of autumn BK sea ice onto the ensemble-mean MSLP from AMIP$_{\mathrm{OBS}}$ (Figure 2c) yields a weak and even opposite pattern in the North Atlantic to that found in reanalysis, with reduced sea ice linked to a weakly positive NAO index. This again implies that the observed relationship between BK sea ice and the NAO could just be a manifestation of internal variability, consistent with the nonstationary of the relationship (Kolstad & Screen, 2019). This result supports the conclusions of Peings (2019), who found a very weak atmospheric response to BK sea ice variability in a high top model. In contrast, the ensemble-mean regression over the North Pacific is similar to that found in reanalysis, suggesting this spatial aspect of the regression onto autumn BK sea ice is forced. When repeating the analysis for each model separately, the regression patterns are highly similar, suggesting a weak dependence on the model used (Figure S1).

When the analysis is repeated for AMIP$_{\mathrm{CLIM}}$, which contains no information about sea ice variability, the same pattern is found as in AMIP$_{\mathrm{OBS}}$ (Figure 2d), including over the North Pacific. This suggests that the forced changes in the North Pacific, which are correlated with BK sea ice variability, are not caused by sea ice variability and, instead, must originate from other aspects of the ocean boundary conditions. The only difference between the ensemble-mean regression in AMIP$_{\mathrm{CLIM}}$ and AMIP$_{\mathrm{OBS}}$ is directly over the BK seas

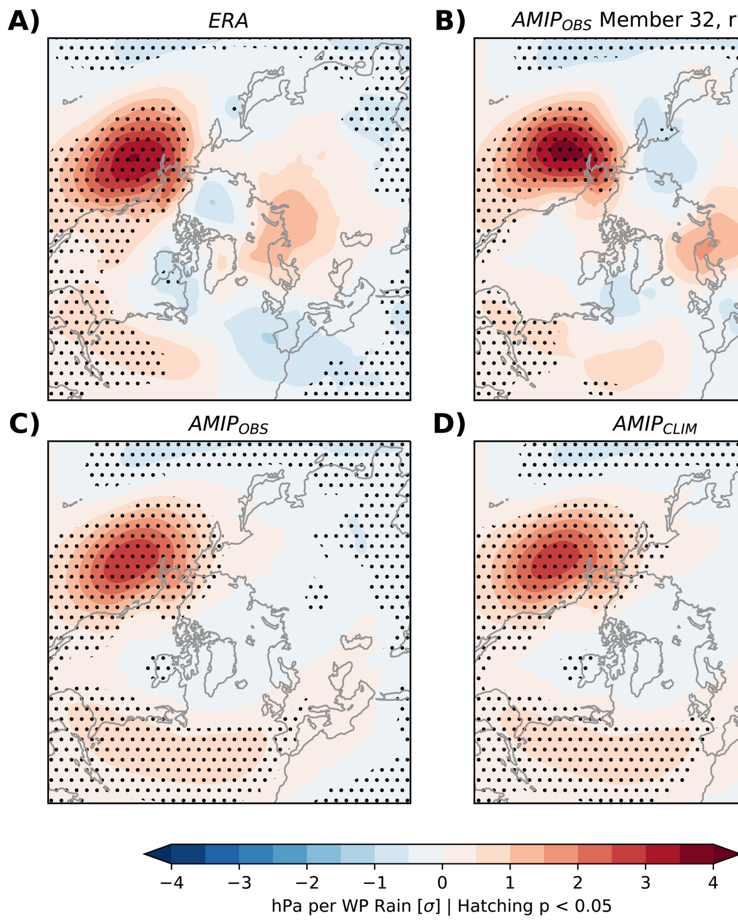

Figure 3. Winter circulation patterns related to preceding tropical Pacific rainfall in reanalysis and model experiments. (a) Linear regression of observed WP_{SO} (standardized) onto DJF MSLP at each grid point in observations, showing the regression coefficient. Stippling is where this regression coefficient is statistically non-zero at the 5% level. (b) Performing the same procedure as (a), except on each individual member in $AMIP_{OBS}$ using that members standardized WP_{SO} rainfall. The member with the strongest latitude-weighted pattern correlation north of 20°N is selected, with the correlation coefficient shown. (c) Same as in (a), except performing analysis on the ensemble mean in $AMIP_{OBS}$. (d) Same as in (a), except for the ensemble mean in $AMIP_{CLIM}$.

region, where in the inclusion of sea ice variability in $AMIP_{OBS}$ leads to enhanced near-surface temperature (not shown) and MSLP variability related to BK sea ice. Additionally, given that Hudson Bay sea ice covaries with BK sea ice, the MSLP above this region is also significantly related to BK sea ice variability.

5. Tropical Origins of Links Between Sea Ice and Winter Circulation

Given the similarity between Figures 2c and 2d, we can infer a minimal causal influence of sea ice on the simulated MSLP regressions onto autumn BK sea ice. This begs the following question: What is the cause of the observed and simulated coverability between autumn BK sea ice and winter MSLP? Given that $AMIP_{ENSO}$ only contains the leading empirical orthogonal function of SST's (i.e., ENSO) and observed sea ice variability and that the latter has minimal effect on the winter circulation in the model, we can use $AMIP_{ENSO}$ to isolate the ENSO influence on the covariability between sea ice and MSLP. The regression of ensemble-mean MSLP from $AMIP_{ENSO}$ onto observed November BK sea ice produces a very similar, albeit weaker (by roughly half over the North Pacific), regression pattern to that in $AMIP_{OBS}$ (not shown). We hypothesize that ENSO, and tropical rainfall variability in general, can partly account for covariability between sea ice and MSLP, especially in the North Pacific.

To further test this hypothesis, we now investigate whether variability in tropical rainfall can partially explain the ensemble-mean regression patterns in Figures 2c and 2d. Preceding tropical West Pacific rainfall (WP_{SO}) is weakly, but statistically significantly, anticorrelated with November BK sea ice ($r = -0.36$, $p < 0.05$) in reanalysis, so we repeat the analysis in Figure 2 but using WP_{SO} rather than November BK sea ice. Note that unlike the case in Figure 2 with sea ice, precipitation is not prescribed and so we perform the regressions onto the simulated WP_{SO} in each ensemble member. Figure 3a shows a strong relationship between the Aleutian Low and WP_{SO} in reanalysis. Given WP_{SO} is increased/decreased during La Niña/El Niño, this confirms the regression pattern related to BK sea ice loss is also related to La Niña. By repeating the regression for each member in $AMIP_{OBS}$ experiments (member WP_{SO} onto member winter MSLP), and performing a weighted linear pattern correlation on the regression patterns north of 20°N, a member is found with the strongest correlation (Member 32, $r = 0.85$; Figure 3b), which reproduces both the spatial pattern and regression strength closely with reanalysis and indicates the model can simulate the observed pattern.

We investigate the forced model relationship between WP_{SO} and the winter circulation by taking the ensemble mean of WP_{SO} in the AMIP experiments and regressing this onto the respective ensemble-mean winter MSLP. The pattern in $AMIP_{OBS}$ and $AMIP_{CLIM}$ is very similar to the ensemble-mean MSLP regression onto BK sea ice (Figures 2c and 2d). Additionally, the relationship is very similar when performed for each model separately (Figure S2). We argue that the apparent relationship between North Pacific MSLP and BK sea ice is primarily a consequence of the anticorrelation between WP_{SO} and BK sea ice and that the variability in the Aleutian Low is forced by tropical variability and not BK sea ice variability. Physical mechanisms that support this teleconnection from the tropical to extratropical Pacific involve divergence/convergence in the upper tropical troposphere, which excite Rossby waves that propagate into the midlatitudes modifying the large-scale circulation (Brönnimann et al., 2007; Garfinkel & Hartmann, 2008; Scaife et al., 2017).

6. Conclusions

Our results provide new evidence in support of the notion that the observed relationship between autumn BK sea ice variability and the winter midlatitude circulation is noncausal. Instead, we argue that this relationship arises in part due to atmospheric internal variability in the Atlantic and in part originates in the tropical Pacific. The former provides a possible, and arguably most likely, explanation for apparent connections between autumn BK sea ice and winter MSLP in the North Atlantic (i.e., NAO). Although individual ensemble members can reproduce a negative NAO-like regression pattern with November BK sea ice, the forced response is weak and different to the apparent response in reanalysis. An important caveat to this work is that we cannot fully rule out that there is a causal link between sea ice and the NAO that models do not faithfully capture (Scaife & Smith, 2018). That said, our conclusion that the forced circulation response to BK sea ice is weak is supported by past work based on various independent data sets and methods (e.g., Blackport et al., 2019; Koenigk et al., 2019; McCusker et al., 2016; Ogawa et al., 2018; Peings, 2019; Sun et al., 2016).

The apparent connection between autumn BK sea ice and winter MSLP in the North Pacific has a forced component. However, this covariability appears to be driven by a third factor: tropical convection in the western Pacific. Autumn tropical rainfall variability in the West Pacific has long been known to affect midlatitude winter circulation in the North Pacific. Here we have argued that the anticorrelation between West Pacific rainfall and BK sea ice leads to covariability between Arctic sea ice and the winter extratropical atmospheric circulation, even in the absence of a causal connection between BK sea ice and the extratropics, which is a novel result. An open question to be explored in future work is whether there is a causal relationship between tropical rainfall and Arctic sea ice.

Acknowledgments
J. W. is supported by a NERC GW4+ Doctoral Training Partnership studentship from the Natural Environment Research Council (NE/L002434/1). We acknowledge the FACTS data, available publicly online (https://www.esrl.noaa.gov/psd/repository/alias/factsdocs), ERA-Interim reanalysis available publicly (https://apps.ecmwf.int/datasets/), and GPCP data available publicly (https://www.esrl.noaa.gov/psd/data/gridded/data.gpcp.html). We also acknowledge useful discussions with Nick Dunstone and Doug Smith.

References

Adler, R. F., Huffman, G. J., Chang, A., Ferraro, R., Xie, P. P., Janowiak, J., et al. (2003). The version-2 Global Precipitation Climatology Project (GPCP) monthly precipitation analysis (1979-present). *Journal of Hydrometeorology*, *4*(6), 1147–1167.

Baxter, I., Ding, Q., Schweiger, A., L'Heureux, M., Baxter, S., Wang, T., et al. (2019). How tropical Pacific surface cooling contributed to accelerated sea ice melt from 2007 to 2012 as ice is thinned by anthropogenic forcing. *Journal of Climate*, *2019*.

Blackport, R., Screen, J. A., van der Wiel, K., & Bintanja, R. (2019). Minimal influence of reduced Arctic sea ice on coincident cold winters in mid-latitudes. *Nature Climate Change*, *9*(9), 697–704.

Brönnimann, S., Xoplaki, E., Casty, C., Pauling, A., & Luterbacher, J. (2007). ENSO influence on Europe during the last centuries. *Climate Dynamics*, *28*(2-3), 181–197.

Cassano, E. N., Cassano, J. J., Higgins, M. E., & Serreze, M. C. (2014). Atmospheric impacts of an Arctic sea ice minimum as seen in the Community Atmosphere Model. *International Journal of Climatology*, *34*(3), 766–779.
Cassou, C. (2008). Intraseasonal interaction between the Madden–Julian oscillation and the North Atlantic Oscillation. *Nature*, *455*(7212), 523.
Collow, T. W., Wang, W., & Kumar, A. (2019). Reduction in northern mid-latitude 2-m temperature variability due to Arctic sea ice loss. *Journal of Climate*, *2019*.
De, B., & Wu, Y. (2019). Robustness of the stratospheric pathway in linking the Barents-Kara Sea ice variability to the mid-latitude circulation in CMIP5 models. *Climate Dynamics*, *53*(1-2), 193–207.
Dee, D. P., Uppala, S. M., Simmons, A. J., Berrisford, P., Poli, P., Kobayashi, S., et al. (2011). The ERA-Interim reanalysis: Configuration and performance of the data assimilation system. *Quarterly Journal of the Royal Meteorological Society*, *137*(656), 553–597.
Dunstone, N., Smith, D., Scaife, A., Hermanson, L., Eade, R., Robinson, N., et al. (2016). Skilful predictions of the winter North Atlantic Oscillation one year ahead. *Nature Geoscience*, *9*(11), 809.
Francis, J. A., & Vavrus, S. J. (2015). Evidence for a wavier jet stream in response to rapid Arctic warming. *Environmental Research Letters*, *10*(1), 014005.
Garfinkel, C. I., & Hartmann, D. L. (2008). Different ENSO teleconnections and their effects on the stratospheric polar vortex. *Journal of Geophysical Research*, *113*, D18114. https://doi.org/10.1029/2008JD009920
Gastineau, G., Garcia-Serrano, J., & Frankignoul, C. (2017). The influence of autumnal Eurasian snow cover on climate and its link with Arctic sea ice cover. *Journal of Climate*, *30*(19), 7599–7619.
Gong, T., Feldstein, S., & Lee, S. (2017). The role of downward infrared radiation in the recent Arctic winter warming trend. *Journal of Climate*, *30*(13), 4937–4949.
Hall, R. J., Scaife, A. A., Hanna, E., Jones, J. M., & Erdelyi, R. (2017). Simple statistical probabilistic forecasts of the winter NAO. *Weather and Forecasting*, *32*(4), 1585–1601.
Henderson, G. R., Barrett, B. S., & Lafleur, D. M. (2014). Arctic sea ice and the Madden–Julian oscillation (MJO). *Climate Dynamics*, *43*(7-8), 2185–2196.
Kelleher, M., & Screen, J. (2018). Atmospheric precursors of and response to anomalous Arctic sea ice in CMIP5 models. *Advances in Atmospheric Sciences*, *35*(1), 27–37.
Kidston, J., Scaife, A. A., Hardiman, S. C., Mitchell, D. M., Butchart, N., Baldwin, M. P., & Gray, L. J. (2015). Stratospheric influence on tropospheric jet streams, storm tracks and surface weather. *Nature Geoscience*, *8*(6), 433.
Kim, B. M., Son, S. W., Min, S. K., Jeong, J. H., Kim, S. J., Zhang, X., et al. (2014). Weakening of the stratospheric polar vortex by Arctic sea-ice loss. *Nature Communications*, *4*, 4646.
Knight, J. R., Maidens, A., Watson, P. A., Andrews, M., Belcher, S., Brunet, G., et al. (2017). Global meteorological influences on the record UK rainfall of winter 2013–14. *Environmental Research Letters*, *12*(7), 074001.
Koenigk, T., Gao, Y., Gastineau, G., Keenlyside, N., Nakamura, T., Ogawa, F., et al. (2019). Impact of Arctic sea ice variations on winter temperature anomalies in northern hemispheric land areas. *Climate Dynamics*, *52*(5-6), 3111–3137.
Kolstad, E. W., & Screen, J. A. (2019). Non-stationary relationship between autumn Arctic sea ice and the winter North Atlantic Oscillation. *Geophysical Research Letters*, *46*, 7583–7591. https://doi.org/10.1029/2019GL083059
Kretschmer, M., Coumou, D., Donges, J. F., & Runge, J. (2016). Using causal effect networks to analyze different Arctic drivers of midlatitude winter circulation. *Journal of Climate*, *29*(11), 4069–4081.
Lee, S. (2012). Testing of the tropically excited Arctic warming mechanism (TEAM) with traditional El Niño and La Niña. *Journal of Climate*, *25*(12), 4015–4022.
Lee, S., Gong, T., Johnson, N., Feldstein, S. B., & Pollard, D. (2011). On the possible link between tropical convection and the Northern Hemisphere Arctic surface air temperature change between 1958 and 2001. *Journal of Climate*, *24*(16), 4350–4367.
Liptak, J., & Strong, C. (2014). The winter atmospheric response to sea ice anomalies in the Barents Sea. *Journal of Climate*, *27*(2), 914–924.
Liu, J., Curry, J. A., Wang, H., Song, M., & Horton, R. M. (2012). Impact of declining Arctic sea ice on winter snowfall. *Proceedings of the National Academy of Sciences*, *109*, 4074–4079.
McCusker, K. E., Fyfe, J. C., & Sigmond, M. (2016). Twenty-five winters of unexpected Eurasian cooling unlikely due to Arctic sea-ice loss. *Nature Geoscience*, *9*(11), 838.
McKenna, C. M., Bracegirdle, T. J., Shuckburgh, E. F., Haynes, P. H., & Joshi, M. M. (2018). Arctic sea ice loss in different regions leads to contrasting Northern Hemisphere impacts. *Geophysical Research Letters*, *45*, 945–954. https://doi.org/10.1002/2017GL076433
Moon, J. Y., Wang, B., & Ha, K. J. (2011). ENSO regulation of MJO teleconnection. *Climate Dynamics*, *37*(5-6), 1133–1149.
Mori, M., Kosaka, Y., Watanabe, M., Nakamura, H., & Kimoto, M. (2019). A reconciled estimate of the influence of Arctic sea-ice loss on recent Eurasian cooling. *Nature Climate Change*, *9*, 123–129.
Mori, M., Watanabe, M., Shiogama, H., Inoue, J., & Kimoto, M. (2014). Robust Arctic sea-ice influence on the frequent Eurasian cold winters in past decades. *Nature Geoscience*, *7*(12), 869.
Neale, R. B., Richter, J. H., Conley, A. J., Park, S., Lauritzen, P. H., Gettelman, A., & Williamson, A. (2010). Description of the NCAR Community Atmosphere Model (CAM 4.0), NCAR Tech. Note NCAR/TN-485+STR, Natl. Cent. for Atmos. Res, Boulder, Colo. https://www.cesm.ucar.edu/models/ccsm4.0/cam/docs/description/cam4_desc.pdf
Neale, R. B., Chen, C. C., Gettelman, A., Lauritzen, P. H., Park, S., Williamson, D. L., et al. (2010). Description of the NCAR community atmosphere model (CAM 5.0). NCAR Tech. Note NCAR/TN-486+STR, (*1*(1), pp1–12).
Nie, Y., Scaife, A. A., Ren, H. L., Comer, R. E., Andrews, M. B., Davis, P., & Martin, N. (2019). Stratospheric initial conditions provide seasonal predictability of the North Atlantic and Arctic Oscillations. *Environmental Research Letters*, *14*(3), 034006.
NOAA ERSL (2019). https://www.esrl.noaa.gov/psd/repository/entry/show?entryid=b507601a-7c2e-482f-948f-7a072559a942&output=wiki.view, accessed 02/09/2019.
Ogawa, F., Keenlyside, N., Gao, Y., Koenigk, T., Yang, S., Suo, L., et al. (2018). Evaluating impacts of recent Arctic sea ice loss on the northern hemisphere winter climate change. *Geophysical Research Letters*, *45*, 3255–3263. https://doi.org/10.1002/2017GL076502
Onarheim, I. H., Eldevik, T., Smedsrud, L. H., & Stroeve, J. C. (2018). Seasonal and regional manifestation of Arctic sea ice loss. *Journal of Climate*, *31*(12), 4917–4932.
Orsolini, Y. J., Senan, R., Benestad, R. E., & Melsom, A. (2012). Autumn atmospheric response to the 2007 low Arctic sea ice extent in coupled ocean–atmosphere hindcasts. *Climate Dynamics*, *38*(11-12), 2437–2448.
Park, H. S., Lee, S., Son, S. W., Feldstein, S. B., & Kosaka, Y. (2015). The impact of poleward moisture and sensible heat flux on Arctic winter sea ice variability. *Journal of Climate*, *28*(13), 5030–5040.

Peings, Y. (2019). Ural blocking as a driver of early-winter stratospheric warmings. *Geophysical Research Letters*, *46*, 5460–5468. https://doi.org/10.1029/2019GL082097

Petoukhov, V., & Semenov, V. A. (2009). A link between reduced Barents-Kara sea ice and cold winter extremes over northern continents. *Journal of Geophysical Research*, *115*, D21111. https://doi.org/10.1029/2009JD013568

Roeckner, E., Bauml, G., Bonaventura, L., Brokopf, R., Esch, M., Giorgetta, M., et al., (2003). The atmospheric general circulation model ECHAM 5. PART I: Model description. Max Planck Institute for Meteorology Rep, 349, 127.

Runge, J., Petoukhov, V., Donges, J. F., Hlinka, J., Jajcay, N., Vejmelka, M., et al. (2015). Identifying causal gateways and mediators in complex spatio-temporal systems. *Nature Communications*, *6*, 8502.

Saha, S., Moorthi, S., Wu, X., Wang, J., Nadiga, S., Tripp, P., et al. (2014). The NCEP climate forecast system version 2. *Journal of Climate*, *27*(6), 2185–2208.

Sardeshmukh, P. D., & Hoskins, B. J. (1988). The generation of global rotational flow by steady idealized tropical divergence. *Journal of the Atmospheric Sciences*, *45*(7), 1228–1251.

Scaife, A. A., Arribas, A., Blockley, E., Brookshaw, A., Clark, R. T., Dunstone, N., et al. (2014). Skillful long range prediction of European and North American winters. *Geophysical Research Letters*, *41*, 2514–2519. https://doi.org/10.1002/2014GL059637

Scaife, A. A., Comer, R. E., Dunstone, N. J., Knight, J. R., Smith, D. M., MacLachlan, C., et al. (2017). Tropical rainfall, Rossby waves and regional winter climate predictions. *Quarterly Journal of the Royal Meteorological Society*, *143*(702), 1–11.

Scaife, A. A., & Smith, D. (2018). A signal-to-noise paradox in climate science. *npj Climate and Atmospheric Science*, *1*(1), 28.

Screen, J. A. (2017). Simulated atmospheric response to regional and pan-Arctic sea ice loss. *Journal of Climate*, *30*(11), 3945–3962.

Smith, D. M., Dunstone, N. J., Scaife, A. A., Fiedler, E. K., Copsey, D., & Hardiman, S. C. (2017). Atmospheric response to Arctic and Antarctic sea ice: The importance of ocean–atmosphere coupling and the background state. *Journal of Climate*, *30*(12), 4547–4565.

Sun, L., Deser, C., & Tomas, R. A. (2015). Mechanisms of stratospheric and tropospheric circulation response to projected Arctic sea ice loss. *Journal of Climate*, *28*(19), 7824–7845.

Sun, L., Perlwitz, J., & Hoerling, M. (2016). What caused the recent "Warm Arctic, Cold Continents" trend pattern in winter temperatures? *Geophysical Research Letters*, *43*, 5345–5352. https://doi.org/10.1002/2016GL069024

Titchner, H. A., & Rayner, N. A. (2014). The Met Office Hadley Centre sea ice and sea surface temperature data set, version 2: 1. Sea ice concentrations. *Journal of Geophysical Research: Atmospheres*, *119*, 2864–2889. https://doi.org/10.1002/2013JD020316

Toniazzo, T., & Scaife, A. A. (2006). The influence of ENSO on winter North Atlantic climate. *Geophysical Research Letters*, *33*, L24704. https://doi.org/10.1029/2006GL027881

Trenberth, K. E., Branstator, G. W., Karoly, D., Kumar, A., Lau, N. C., & Ropelewski, C. (1998). Progress during TOGA in understanding and modeling global teleconnections associated with tropical sea surface temperatures. *Journal of Geophysical Research*, *103*, 14,291–14,324.

Vihma, T. (2014). Effects of Arctic sea ice decline on weather and climate: A review. *Surveys in Geophysics*, *35*(5), 1175–1214.

Wang, L., Ting, M., & Kushner, P. J. (2017). A robust empirical seasonal prediction of winter NAO and surface climate. *Scientific Reports*, *7*(1), 279. https://doi.org/10.1038/s41598-017-00353-y

Woods, C., & Caballero, R. (2016). The role of moist intrusions in winter Arctic warming and sea ice decline. *Journal of Climate*, *29*(12), 4473–4485.

Woods, C., Caballero, R., & Svensson, G. (2013). Large-scale circulation associated with moisture intrusions into the Arctic during winter. *Geophysical Research Letters*, *40*, 4717–4721. https://doi.org/10.1002/grl.50912

Yang, S., & Christensen, J. H. (2012). Arctic sea ice reduction and European cold winters in CMIP5 climate change experiments. *Geophysical Research Letters*, *39*, L20707. https://doi.org/10.1029/2012GL053338

Zhang, P., Wu, Y., Simpson, I. R., Smith, K. L., Zhang, X., De, B., & Callaghan, P. (2018). A stratospheric pathway linking a colder Siberia to Barents-Kara Sea ice loss. *Science Advances*, *4*(7), 6025.